

Received: 13 April 2019 • Accepted: 15 July 2019

Research

doi:10.22034/jcema.2019.201428.1002

Evaluation of Seismic Behavior of Bridges under Effect of Abutment Modeling

Behzad Haseli

Department of Civil Engineering, Kharazmi University, Tehran, Iran.

* Correspondence should be addressed, Department of Civil Engineering, Kharazmi University, Tehran, Iran. Tel: 09373971292; Fax: +9888923503 Email: b.haseli@yahoo.com

ABSTRACT

These Bridges are vital part of the transportation network Department of Civil Engineering. Their destruction caused by the occurrence of a strong earthquake can cause irreparable damages to the regional economy. One of the effective factors on seismic response of a bridge is abutment and its modelling. In most cases, analysis of seismic behavior and modelling of bridges is done using simplifying assumptions. This simplification may cause major changes in prediction of seismic behavior of bridges. Using simplified, roller and full models for abutment is very important in design and evaluation of seismic behavior of bridges. Backfill is a vital factor in modelling abutments. In this study, abutments were analyzed in three scenarios under records related to three stations of Imperial Valley earthquake (1979) and responses compare in two states with and without backfill. The results showed that minimum response (for deck, pier column and abutment) were related to the first modelling scenario (roller abutment) and maximum response were related to the fifth modelling scenario (simplified abutment as suggested by Shamsabadi for cohesive soil). Modelling of backfill was effective on displacement and rotation of pier column and displacement of deck and moment of abutment. For all records of earthquake, wall pier abutment (sixth scenario) was considerably consistent with modelling based on Caltrans guideline for sandy soil (second scenario). In height ranging from 5 to 9 meters, the suggested modelling (wall pier abutment) can be used instead of Caltrans method. In this height range, the results (maximum abutment displacement and abutment pressure) vary from 11 to 23%.

Keywords: abutment modelling, soil-abutment interaction, abutment stiffness, roller abutment, simplified abutment.

Copyright © 2019 Behzad Haseli This is an open access paper distributed under the [Creative Commons Attribution License](https://creativecommons.org/licenses/by/4.0/). Journal of Civil Engineering and Materials Application is published by [Pendar pub](http://www.pendarpub.com); Journal p-ISSN 2676-232X; Journal e-ISSN 2588-2880.

1. INTRODUCTION

One of the effective factors on seismic response of bridges is abutment and its modeling. Seismic responses of different parts of a bridge modeled by considering soil hardness will be considerably different from the case where abutments are modeled a roller or simplified abutments [1, 2]. Hence, there are different methods for modeling abutments, such as:

1. Roller abutment
2. Spring abutment
3. Simplified abutment using linear springs
4. Complete abutment
5. Abutment modeling by considering the effect of soil-abutment interactions

Abutments are suitable for conveying forces of inertia at the time of the earthquake. Abutments are designed by considering governing principles of retaining walls based on soil resistant and active pressure theory. Most studies conducted on seismic response of bridges are related to dynamic behavior of bridge deck; little is known about

the role of abutments in seismic response of bridges. Under San Fernando earthquake in 1971, it was found that resistance provided by abutment back wall has an important influence on dynamic behavior of some bridges [1]. Douglas and Davis (1946) suggested relations to calculate initial stiffness of rectangular abutment back wall [2]. In 1988, Wilson presented a relation to calculate maximum displacement of abutment back wall vertically and to calculate stiffness of abutment vertically [3]. These relations were used by Duncan and Mokwa (2001) to estimate stiffness of piles [4]. To study on the effects of different parts of resistant bridges under earthquake, important studies were conducted by Megally and Zheng. By conducting large-scale experiments, Megally et al. (2001) presented a non-linear model for interior and exterior shear keys on abutments. Based on abutment back wall, Shamsabadi (2010) [5] calculated maximum displacement of abutment and determined equivalent hardness of backfill considering

the type of embankment and lateral forces [1,5]. Stiffness of abutments applied in modeling of bridges will be different depending on the type of the back wall and the model used to simulate the performance of the abutment. Therefore, it is particularly important to consider the type of back wall in abutment modeling [6]. Gao and Lin perused the effects of modeling parameters on the seismic analysis of bridges [7]. Taherkhani, in an article studied bridge abutment displacement constructed on piles and geogrid reinforced soil using the finite element method [8]. Xie perused Probabilistic models of abutment backfills for regional seismic assessment of highway bridges in California [9]. Paolo Zampieri perused Seismic capacity of masonry arches with irregular abutments and arch thickness [10]. Chern Kun Estimation of response of skewed bridges considering pounding and supporting soil [11]. Zakeri, in an article, preused Design of bridges with skewed abutments for a target tolerable seismic loss [12]. Kozak study Seismic modeling of integral abutment bridges in Illinois [13].

2. MATERIALS AND METHODS

Various studies have suggested different methods for calculating stiffness considering the type of embankment [1, 5 and 17]. This study evaluates a three-span concrete bridge with simple spans. Roller and simplified abutments are modeled by considering stiffness of the soil around the abutment (wall pier). The relations proposed by Wilson (1988) are used to calculate vertical stiffness [18]. The studied bridge has a symmetrical two-way road; the two lanes are 1.2 m away from each other. The bridge is 97.54 m in length. The bridge has two end spans (30.48 m in length) and one intermediate span (36.58 m in length). The bridge has two reinforced concrete bents and each bent has three columns. Columns are circular with a diameter of 1.2 m [19]. The superstructure of the studied bridge is

Nasiri and Zarfam in a research studied the loading pattern factor of modal pushover analysis for integrated bridges using IDA responses [14]. Joseph Fox in an article studied Acceleration Response of a Geosynthetic Reinforced Soil Bridge Abutment under Dynamic Loading [15]. Elena Meteş and el perused integral bridges length limitation, transition slabs [16]. This study compares seismic behavior of a bridge modeled by different abutment modeling under several near-field earthquake records including effects of forward, backward and neutral directivity. A method is suggested for determining equivalent stiffness of abutment considering the effect of soil around the abutment by defining and analyzing wall piers in situ using Mononobe-Okabe method. The analysis used in this study is time history analysis. Results of analysis include total displacement and rotation of backfill and pier column in the longitudinal direction, maximum displacement and pressure of abutment.

composed of six steel summer beams spaced 2.3 m center to center and a concrete slab (20 cm thick). Cap beam is used at junction of bents to bridge deck. Cap beam is installed in a rectangular form (0.2 m in thickness) where bents are located between the deck and bases. For validation of the bridge structure, the studied bridge is modeled with a model developed by the Federal Highway Administration No. 4 (FHWA04-1996) and Kim and Elnashai [19,20]. Its period is calculated and compared to the equivalent period obtained by Kim and Elnashai. As shown in Table 1, period of the bridge modeled in this study is slightly different (1.4%) from the bridge modeled by Kim and Elnashai.

2.1. METHODS AND SELECTION CRITERIA OF EARTHQUAKE RECORD

One Soil of the bridge site studied is soil type C of AASHTO [8, 21]. Hence, average shear wave velocity to 30 m depth (V_{s30}) from the ground is within average shear wave velocity of soil type C (375-700 m/s) for each accelerogram. Earthquake records are obtained from Pacific Earthquake Engineering Research (PEER) database. All pairs of horizontal accelerograms selected in

Table 2 are scaled by scaling method suggested in Publication 463 [9], as shown in Table 3. Based on Bozorgnia et al. [22,23], response spectrum of vertical component in 20, 10, 5 and 40 km from the fault is 0.75, 0.65, 0.57 and 0.52 times greater than horizontal component, respectively.

2.2. ABUTMENT MODELLING-ROLLER ABUTMENT

This modelling approach directly uses stiffness of neoprene designed by considering the sizes intended [24], because neoprene and roller are equivalent and show a similar performance. For modelling neoprene at the site of abutments, finite elements of the spring interface are used by considering linear behavior [25]. Sizes of the neoprene used (in meters), as shown in Table 4, are considered similar for both abutments. In Table 4, a, b and t represent length, width and thickness of the neoprene, respectively. Longitudinal stiffness is equal to transverse stiffness ($K_t = K_l$); stiffness in both directions corresponds to shear

Modulus (G) [equation1]. Vertical stiffness (K_v) corresponds to modulus of elasticity (E) [equation2]. Table 9 summarizes the results.

$$K_v = \frac{Eab}{t} \quad (1)$$

$$K_t = K_l = \frac{Gab}{t} \quad (2)$$

2.3. SIMPLIFIED ABUTMENT-ABUTMENT MODELING BASED ON CALTRANS, DENSE SAND BACKFILL

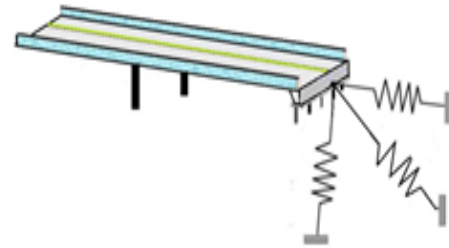
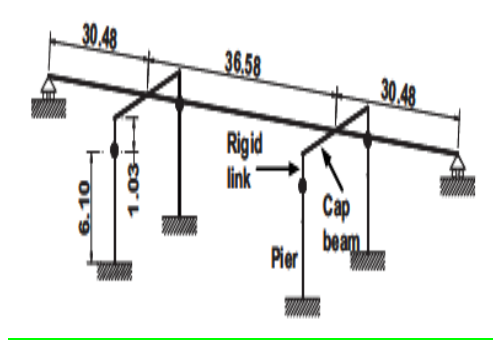
According to Caltrans [17, 26], equivalent stiffness of the abutment is expressed as follows based on maximum

displacement of the backfill considering height of the back wall [equation 3, 4, 5]:

$$Ae = h * w \tag{3}$$

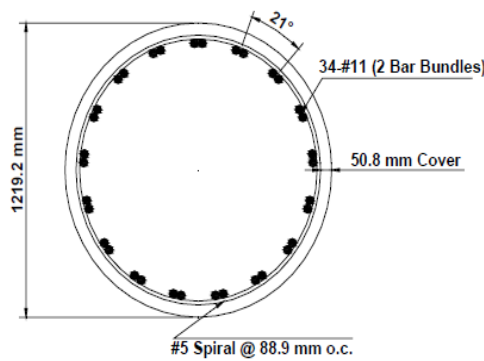
$$Kab_u = \frac{Pabu}{\Delta_{eff}} = \frac{Pabu}{\Delta_{max}} \tag{5}$$

$$Pw = Ae * 239 * \frac{h}{1.7} \tag{4}$$



(a) Analytical model of the modeled bridge

(b) Abutment details



(C) pier section details

Figure 1. Analytical model of the modeled bridge and details[20]

Table 1. The period obtained by SAP and calculated by Kim and Elnashai

| Period (T) obtained by Kim and Elnashai | Period (T) obtained by SAP | Difference (%) |
|---|----------------------------|----------------|
| 0.3515 | 0.3565 | 1.4% |

Table 2. Accelerograms related to three stations of Imperial Valley earthquake

| Earthquake | Year | Vs30(m/s) | Magnitude | Station | Mechanism |
|-------------------------------|------|-----------|-----------|-------------------------|-------------|
| Imperial valley (AGR) | 1979 | 242.05 | 6.53 | Agrarians | Strike slip |
| Imperial valley (CXO) | 1979 | 231.23 | 6.53 | Calexico | Strike slip |
| Imperial valley (Elcentro-07) | 1979 | 210.51 | 6.53 | Imperial valley college | Strike slip |

Table 3. Scale factor for the selected horizontal and vertical components

| Earthquake | SFL&SFT | Sv |
|-------------------------------|---------|--------|
| Imperial valley (AGR) | 1.37 | 1.0275 |
| Imperial valley (CXO) | 1.34 | 0.764 |
| Imperial valley (Elcentro-07) | 1.27 | 0.952 |

Table 4. Sizes of the neoprene used

| | a (m) | b (m) | t (m) |
|---------------|-------|-------|-------|
| Abutment 1, 2 | 0.3 | 0.2 | 0.53 |

Table 5. Maximum displacement by considering type of backfill as suggested in Caltrans

| Type of backfill | Δmax |
|-------------------------------------|-------|
| Dense sand | 0.01h |
| Semi-dense sand and compressed silt | 0.02h |
| Loose gravel | 0.04h |
| Clay | 0.05h |

Where A_e is an effective Area of abutment of bridge, h , is height of abutment, w is effective width of abutment, P abut is effective force in abutment of bridge, Δ_{eff} is maximum displacement in abutment of bridge and K abut is equal stiffness in abutment of bridge [17]. The maximum displacement of the abutment is given in equation 5, for four different soil modes by suggested in Caltrans presented in Table 5. In this case, the embankment is made of dense sand. To calculate vertical stiffness of abutment considering back wall, Wilson and

Plose [27, 28] used following equation 6:

$$\delta_z = \frac{(1 - \gamma^2)}{Es} P b l \tag{6}$$

Where, modulus of elasticity, Poisson's ratio and shape factor are evident; p represents lateral force at the unit - Level and b is backfill width. Given the sizes of backfill, shape factor is obtained as shown in Table 6 [18].

Table 6. Shape factor with regard to sizes of backfill

| L/B | Shape Factor(l) |
|-----|-----------------|
| 1 | 0.8 |
| 5 | 1.7 |
| 10 | 2 |

2.4. ABUTMENT MODELLING BASED ON CALTRANS, SEMI-DENSE SAND AND COMPRESSED SILT BACKFILL

According to Caltrans criteria presented in section 3.2.1, longitudinal (Kl), transverse (Kt) and vertical (Kv) stiffness are calculated as shown in Table 9 [17, 26]. In

this case the embankment is made of semi-dense sand and compressed silt.

2.5. ABUTMENT MODELLING BASED ON SHAMSABADI, GRANULAR BACKFILL

Shamsabadi [5] suggested relations for determining longitudinal stiffness of abutments considering the type of backfill. These relations are based on lateral force per unit width of backfill (F) and lateral displacement (y) [equation 7]:

$$F_y = \frac{ay}{1 + by} \left(\frac{H}{Hr}\right)^n \tag{7}$$

Given the type of backfill and the considered height and sizes, a , b and n are calculated as shown in Table 7. In this

case, the embankment is made of granular soil. Using the above value of exponent n , we perform a secondary minimization problem to estimate a and b . For a given value of n and back wall height H , we compute the complete lateral response backbone curve of an abutment with either Granular or Cohesive backfill—up to y_{max} . In equation (7), F_y = lateral force per unit width of the back wall .at lateral displacement y ; a and b =two new parameters that you get from table7 and (H/Hr) =back wall height factor in which H is the back wall height, Hr is the reference back wall height henceforth chosen to be $Hr=1$ m and n is a dimensionless exponent [5].

Table 7. Constant coefficients of Shamsabadi's relation

| Site/backfill H(m) | Granular | | | Cohesive | | |
|-----------------------|-------------|----------|------|-------------|----------|------|
| | a (KN/cm/m) | b (1/cm) | n | a (KN/cm/m) | b (1/cm) | n |
| 1 | 410.6 | 1.867 | 1.56 | 249.1 | 0.8405 | 1.05 |
| 1.25 | 316.6 | 1.468 | 1.56 | 199.4 | 0.6755 | 1.05 |
| 1.50 | 258.4 | 1.206 | 1.56 | 166.1 | 0.5637 | 1.05 |
| 1.67 | 230.8 | 1.073 | 1.56 | 149.6 | 0.5084 | 1.05 |
| 1.75 | 218.5 | 1.020 | 1.56 | 142.9 | 0.4856 | 1.05 |
| 2 | 190.2 | 0.8836 | 1.56 | 125.6 | 0.4270 | 1.05 |
| 2.25 | 168.7 | 0.7784 | 1.56 | 112.2 | 0.3811 | 1.05 |
| 2.50 | 152.8 | 0.6954 | 1.56 | 101.6 | 0.3446 | 1.05 |

As suggested by Shamsabadi, maximum displacement occurred in the backfill is calculated, as shown in [Table 8](#).

Table 8. maximum displacement of backfill as suggested by Shamsabadi

| y _{max} /H | backfill |
|---------------------|----------|
| 0.05 | Granular |
| 0.1 | Cohesive |

Given the lateral force and maximum displacement of the backfill, stiffness of the abutment is calculated by

Hook's relation, as shown in Table 9 [\[17, 26\]](#).

2.5. ABUTMENT MODELLING BASED ON SHAMSABADI, COHESIVE BACKFILL

In this case, the effect of back wall is applied on ultimate stiffness of the abutment. Therefore, static pressure and dynamic pressure of the back wall [equation 12] cause displacement of the wall pier. Finally, equivalent stiffness of the abutment is calculated at the presence of the force applied on the wall pier and displacement calculated by the software. In this study, the back wall is assumed dry sand. For critical slip surface, soil drift on the non-cohesive back wall is expressed as follows [\[25, 29\]](#):

passive earth pressure coefficient (calculated by equation 11), H=wall height and kv=pseudo static acceleration factor.

$$K_{pe} = \frac{\cos(\phi - \theta - \phi)^2}{\cos \theta^2 \cos \phi \cos(\delta + \phi + \theta) \left[1 + \sqrt{\frac{\sin(\delta + \phi) \sin(\phi - \beta - \phi)}{\cos(\delta + \beta + \phi) \cos(\beta - \theta)}} \right]}$$

$$P_p = 0.5 K_p \gamma H^2 \tag{8}$$

Total passive pressure (PpE) can be divided into static (Pp) and dynamic (ΔPpE) components [\[27\]](#):

$$K_p = \frac{\cos(\phi - \theta)^2}{\cos \theta^2 \cos(\delta + \theta) \left[1 + \sqrt{\frac{\sin(\delta + \phi) \sin(\phi - \beta - \phi)}{\cos(\phi + \theta) \cos(\beta - \theta)}} \right]}$$

$$P_{pE} = P_p + \Delta P_{pE} \tag{12}$$

Where, Pp=passive capacity of a retaining wall per unit width; γ=unit weight of the backfill soil; KP=coefficient of maximum passive earth pressure; H=wall height and δ represents friction angle at the interface between the wall and soil. According to Okabe (1926) and Mononobe (1929), total active drift is expressed similarly to quasi-static drift [\[30, 31\]](#):

Seed and Vitman (1970) suggested that ΔPpE could be considered as about 0.6 of height from the base of the wall. Displacement caused by in the highest point of the retaining wall is calculated using SAP software. Finally, equivalent longitudinal stiffness is calculated for the retaining wall at the abutment at the presence of total lateral force and maximum displacement created. Using constant coefficients, Maroni and Chai (1994) converted the longitudinal response to transverse response. Thus, longitudinal stiffness of abutment and resistance of the end wall (Kl) is converted to transverse stiffness of abutment and resistance of the end wall (Kt) using impact factor of the wall (CL=2/3) and participation factor of the wall (CW=4/3) [\[32, 33\]](#). Longitudinal displacement is 14.5 cm. Given the relations above, longitudinal (Kl), transverse (Kt) and vertical (Kv) stiffness are calculated, as shown in [Table 9](#).

$$P_{pe} = 0.5 K_{pe} \gamma H^2 (1 - K_v) \tag{10}$$

Where, Ppe = total passive capacity of a retaining wall per unit width; γ=unit weight of the backfill soil; Kpe=

Table 9. Longitudinal, transverse and vertical stiffness in the six model

| | Kl(ton/m) | Kt(ton/m) | Kv(ton/m) |
|-------------------|---------------|---------------|---------------|
| Abutment# model 1 | $1.2 * 10^4$ | $1.2 * 10^4$ | $2.9 * 10^4$ |
| Abutment# model 2 | $1.24 * 10^5$ | $1.10 * 10^5$ | $3.7 * 10^5$ |
| Abutment# model 3 | $6.23 * 10^4$ | $5.54 * 10^4$ | $3.7 * 10^5$ |
| Abutment# model 4 | $1.2 * 10^3$ | $0.10 * 10^3$ | $3.7 * 10^5$ |
| Abutment# model 5 | $0.29 * 10^3$ | $0.26 * 10^3$ | $3.7 * 10^5$ |
| Abutment# model 6 | $1.29 * 10^5$ | 0 | $7.46 * 10^5$ |

Table 10. The details of structural models considered in the analyses

| Model case | Properties (with backfill) |
|-------------------|---|
| Abutment# model 1 | Roller Abutment: This modeling approach directly uses stiffness of neoprene |
| Abutment# model 2 | Abutment Modeling Based on Caltrans, Dense Sand Backfill |
| Abutment# model 3 | Abutment Modeling Based on Caltrans, Semi-dense Sand and Compressed Silt Backfill |
| Abutment# model 4 | Abutment Modeling Based on Shamsabadi, Granular Backfill |
| Abutment# model 5 | Abutment Modeling Based on Shamsabadi, Cohesive Backfill |
| Abutment# model 6 | Wall Pier Abutment Modeling: In this case, effect of back wall is applied on ultimate stiffness of the abutment |

3. RESULT AND DISCUSSION

One of the most accurate and most reliable analyses used for structures (buildings and bridges) is non-linear time history analysis used to achieve accurate solutions. This study performs non-linear time history analysis on 6 bridges modeled with different abutments.

Abutment modeling and the selected earthquake record (forward (ELC), neutral (CXO) and backward (AGR) directivity) will considerably influence seismic responses of the bridge. Figures 5, 6 and 7 shows longitudinal displacement pier column and Figures 8, 9 and 10 shows Longitudinal deck displacement of bridge. Displacement curves show that maximum displacement occurs in the fifth scenario and minimum displacement occurs in the first scenario under all records (Figures 5 to 10). In all

scenarios, displacement of the pier column and deck without backfill is higher than displacement of the pier column and deck with backfill. Figures 11, 12 and 13 shows longitudinal rotation pier column of bridge. These figures shows that maximum rotation occurs in the fifth scenario. It is observed that regardless of the effect of the backfill increase value rotation in all scenarios. Figures 14, 15 and 16 shows Maximum Abutment Moment of bridge. The additive procedure due to the regardless of the backfill effects is observed in the case of displacement of the pier column and deck, but in the case of maximum abutment moment, the responses are higher in position of considering the effects of the backfill.

3.1. EFFECT OF ABUTMENT MODELLING ON PIER COLUMN AND DECK DISPLACEMENT

The main cause of difference in displacement of deck and pier column is different stiffness of these two elements. Stiffness of pier column is lower than stiffness of deck. As a result, displacement of pier column is higher than displacement of deck and abutments (according figures 5 to 10). Obviously, displacement of the deck under ELC record is higher than other records due to forward directivity. As shown in Fig 2,3 and 4, the highest

difference between maximum and minimum longitudinal displacement of pier column is observed in model 1 and model 5. This difference in response is equal to 18% (with backfill) and 20.6% (No backfill). Moreover, the least difference between maximum and minimum longitudinal displacement of pier column is observed in model 4 and model 6. This difference in response is equal to 2% (with backfill) and 2.6% (No backfill).

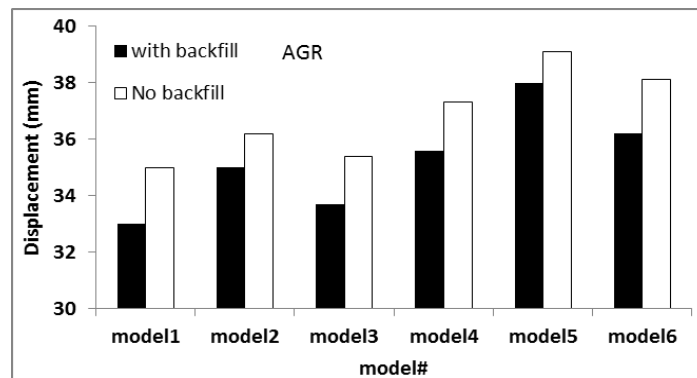


Figure 2. Longitudinal pier column displacement under AGR record

From Fig 5, 6 and 7 observed that the highest difference between maximum and minimum longitudinal

displacement of deck is observed in model 1 and model 5. This difference in response is equal to 20.7% (with

backfill) and 14.8% (No backfill). Moreover, the least difference between maximum and minimum longitudinal displacement of deck is observed in model 4 and model 6.

The difference between the results in this case is less than 2% (in both cases, the backfill).

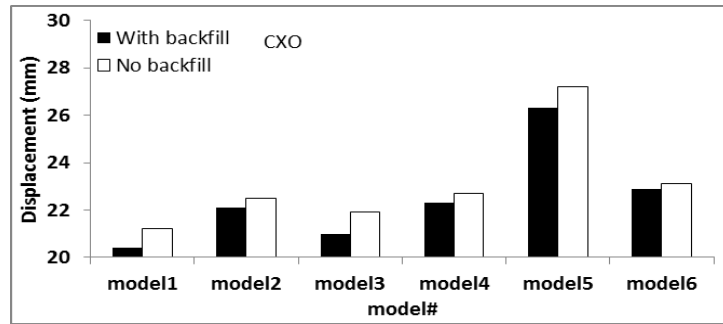


Figure 3. Longitudinal pier column displacement under CXO record

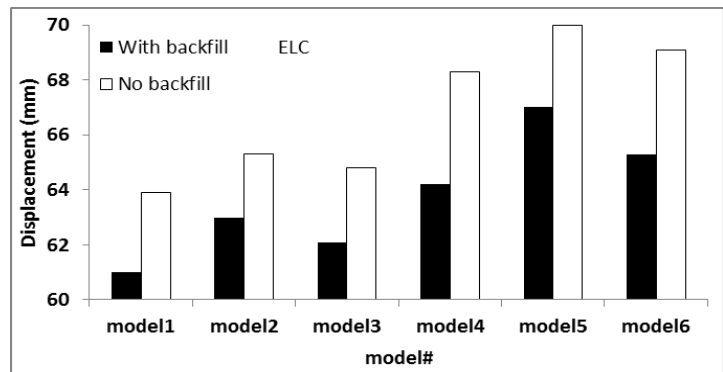


Figure 4. Longitudinal pier column displacement under ELC record

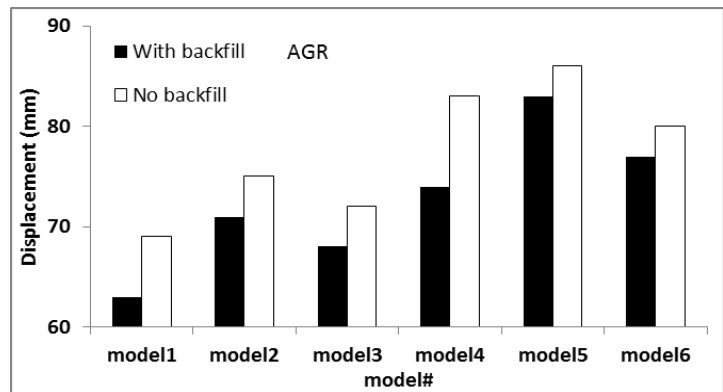


Figure 5. Longitudinal deck displacement under AGR record

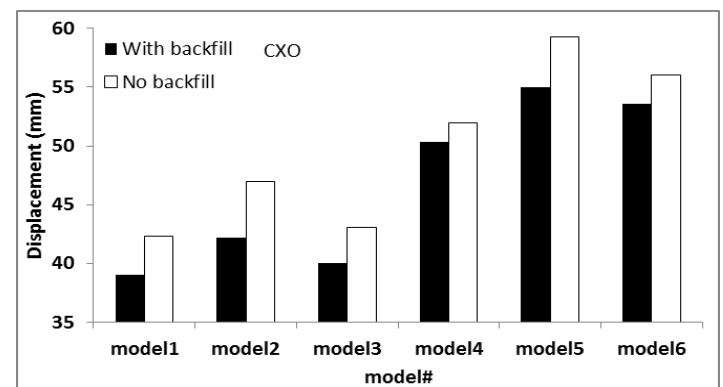


Figure 6. Longitudinal deck displacement under CXO record

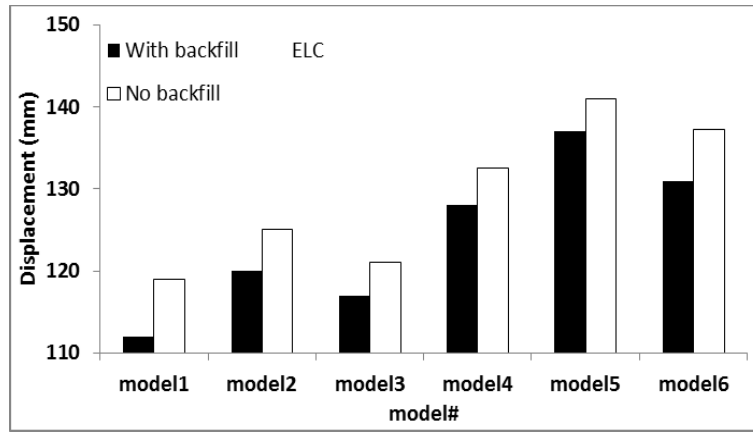


Figure 7. Longitudinal deck displacement under ELC record

3.2. EFFECT OF ABUTMENT MODELLING ON ROTATION PIER COLUMN AND ABUTMENT MOMENT

As shown in Fig 8, 9 and 10 the highest difference between maximum and minimum longitudinal rotation of pier column is observed in model 1 and model 5. This difference in response is equal to 86% (with backfill) and 83% (No backfill). Moreover, the least difference

between maximum and minimum longitudinal displacement of pier column is observed in model 4 and model 6. This difference in response is equal to 2% (with backfill) and 2.6% (No backfill).

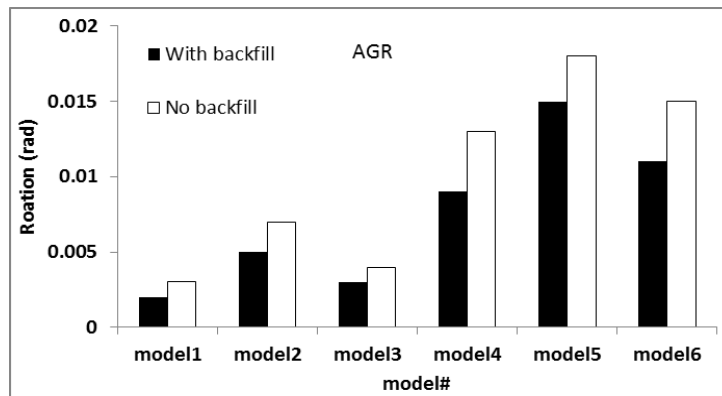


Figure 8. Longitudinal rotation pier column under AGR record

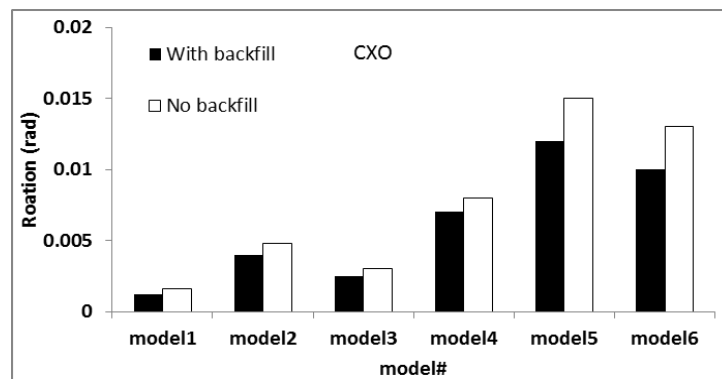


Figure 9. Longitudinal rotation pier column under CXO record

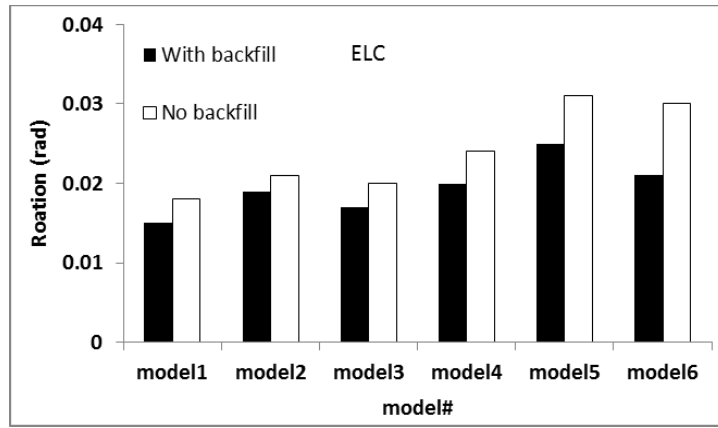


Figure 10. Longitudinal rotation pier column under ELC record

As shown in Fig 11, 12 and 13, the maximum abutment moment recorded in the fifth and the lowest abutment moment is achieved in the first case. The maximum abutment moment is observed when considering the

effects of the backfill cause increase in response. So that the maximum abutment moment in modelling abutment with backfill has increased by 10%.

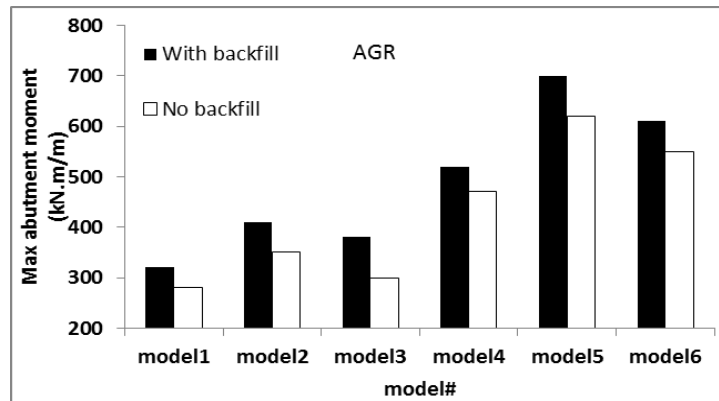


Figure 11. Max abutment moment in six modeling scenarios under AGR record

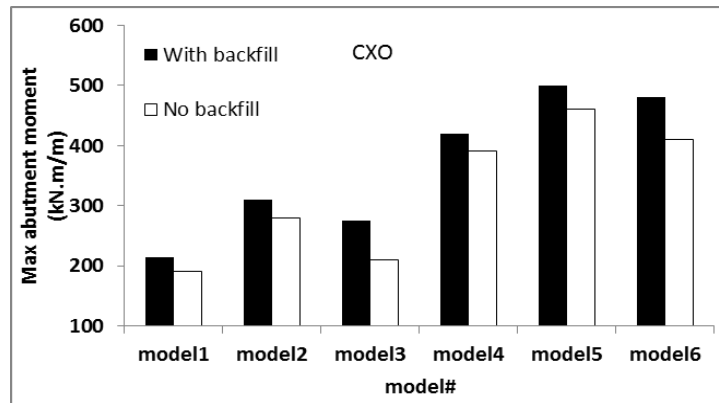


Figure 12. Max abutment moment in six modeling scenarios under CXO record

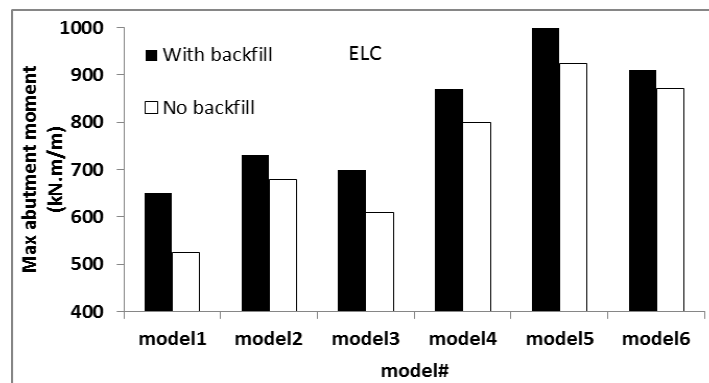


Figure 13. Max abutment moment in six modeling scenarios under ELC record

3.3. EFFECT OF ABUTMENT MODELLING ON DISPLACEMENT AND PRESSURE ABUTMENT

Figures 14, 15 and 16 compare maximum displacement of the abutment and figures 17, 18 and 19 compare abutment pressure for different heights of the back wall under records of three seismic stations of Imperial Valley earthquake (1979). It is observed that at the height 0-5m, the maximum displacement and pressure behind abutment are equal in all modelling abutment modes, but from height 5m onwards, by increasing the height of abutment, displacement and pressure in different modes of modelling are interdependent. By increasing abutment height, the trend of changes in maximum displacement is ascending. By increasing backfill height, equivalent stiffness of the abutment increases. At the height 5-9 m,

the difference in displacement and abutment pressure is 11-23% in the two models 2 and 6. At this height, the wall pier modelling can be a good alternative for Caltrans guideline. Therefore, the applicable range of the wall pier modelling can be presented based on maximum wall displacement to its height considering the type of backfill (assuming dense sand), as shown in Table 11. As shown in Figures 17, 18 and 19, displacement caused by wall pier abutment modelling (sixth scenario) is consistent with results based on Caltrans guideline (second and third scenario).

Table 11. Comparison of applicable range of wall pier modelling and Caltrans guideline

| State of modeling | y/H |
|-----------------------|-------|
| Caltrans | 0.01 |
| Wall pier(new method) | 0.018 |

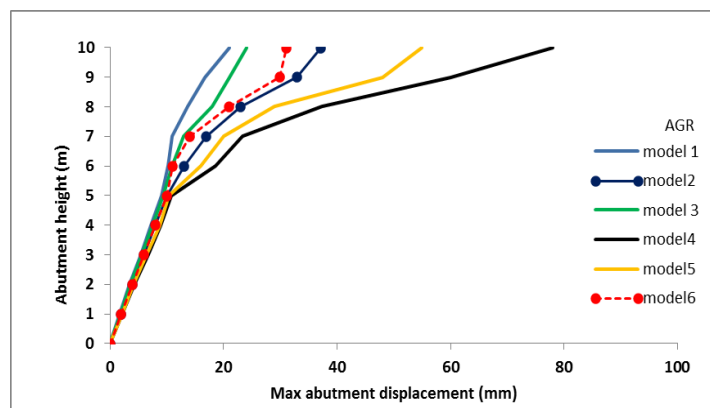


Figure 14. Maximum abutment displacement under AGR record

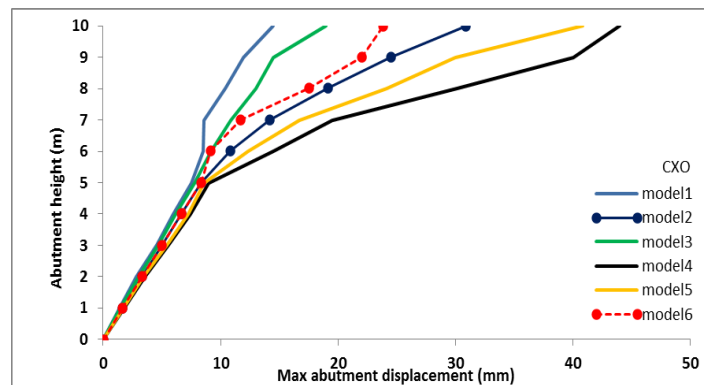


Figure 15. Maximum abutment displacement under CXO record

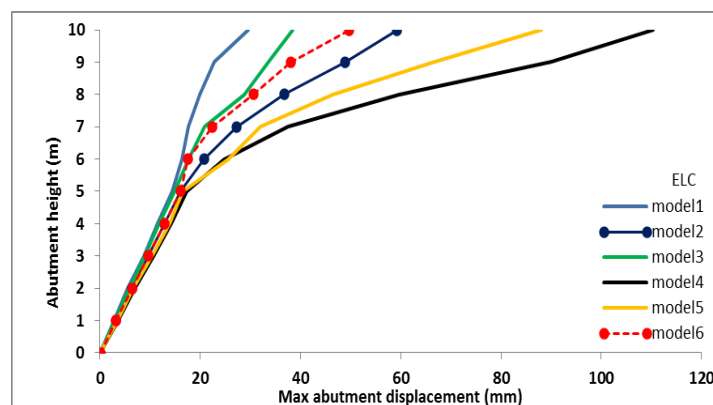


Figure 16. Maximum abutment displacement under ELC record

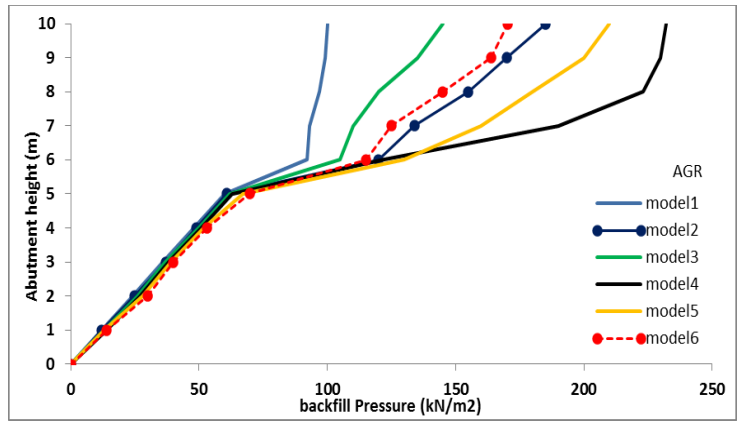


Figure 17. Abutment pressure under AGR record

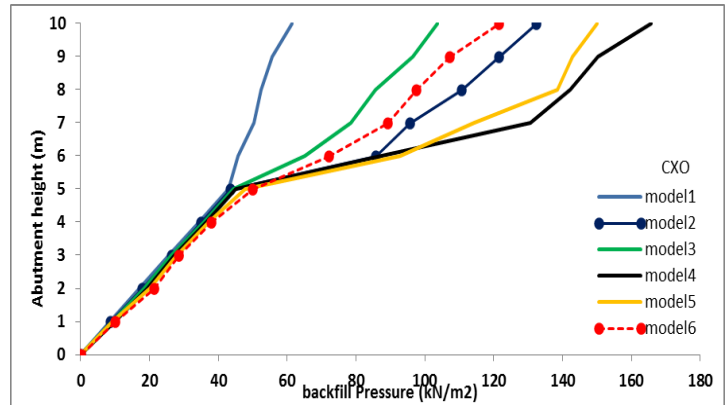


Figure 18. Abutment pressure under CXO record

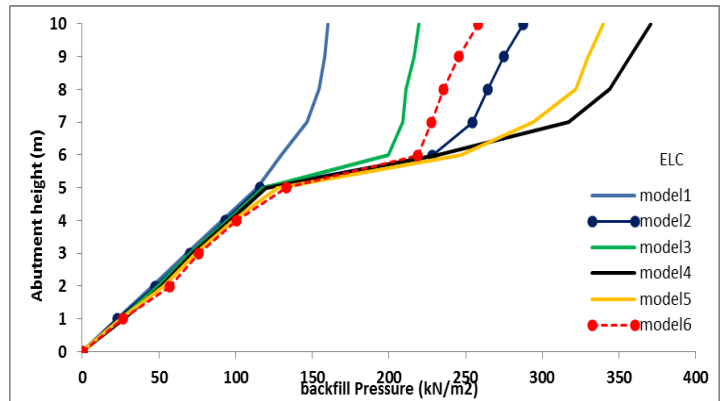


Figure 19. Abutment pressure under ELC record

4. CONCLUSION

A Most of the responses were modeled in the fifth case and the lowest responses were obtained in the first model, so that difference between maximum and minimum displacement of pier column is equal to 18% (with backfill) and 20.6% (No backfill) and difference between maximum and minimum displacement of deck is equal to 20.7% (with backfill) and 14.8% (No backfill). The difference between maximum and minimum rotation of pier column is equal to 86% (with backfill) and 83% (No backfill). Retraction of the effects of backfill increases the response, but in the case of abutment moment, the reverse conditions are the opposite. So that the maximum moment in modelling abutment with backfill has increased by 10%. The increase in height of the back wall increase displacement and pressure. For all records of earthquake, results of the wall pier modeling (sixth scenario) are remarkably consistent with Caltrans guidelines for sandy

soil (second scenario). Therefore, displacements of these methods are accurately consistent when back wall height ranges from 5 to 9 m. At the height 5-9 m, the difference in displacement and abutment pressure is 11-23% in the two models wall pier modeling (sixth scenario) and Caltrans guidelines for sandy soil (second scenario). At this height, the wall pier modeling can be a good alternative for Caltrans guideline. Therefore, the applicable range of the wall pier modeling can be presented based on maximum wall displacement to its height considering the type of backfill (assuming dense sand). At this height, the suggested modeling (wall pier abutment) can be used instead of Caltrans modeling. Backfill-abutment interaction is more evident in the sixth scenario under AGR record compared to other scenarios.

FUNDING/SUPPORT

Not mentioned any Funding/Support by authors.

AUTHORS CONTRIBUTION

This work was carried out in collaboration among all authors.

ACKNOWLEDGMENT

Not mentioned by authors.

CONFLICT OF INTEREST

The author (s) declared no potential conflicts of interests with respect to the authorship and/or publication of this paper.

5. REFERENCES

- [1] Rollins KM, Cole RT. Cyclic lateral load behavior of a pile cap and backfill. Journal of geotechnical and geoenvironmental engineering. 2006 Sep 01;132(9):1143-1153. [\[View at Google Scholar\]](#); [\[View at Publisher\]](#).
- [2] Douglas DJ, Davis EH. The movement of buried footings due to moment and horizontal load and the movement of anchor plates. Geotechnique. 1964 Jun 1;14(2):115-132. [\[View at Google Scholar\]](#); [\[View at Publisher\]](#).
- [3] Wilson JC. Stiffness of non-skew monolithic bridge abutments for seismic analysis. Earthquake engineering & structural dynamics. 1988 Aug 1;16(6):867-883. [\[View at Google Scholar\]](#); [\[View at Publisher\]](#).
- [4] Duncan JM, Mokwa RL. Passive earth pressures: theories and tests. Journal of Geotechnical and Geoenvironmental Engineering. 2001 Mar 01;127(3):248-257. [\[View at Google Scholar\]](#); [\[View at Publisher\]](#).
- [5] Shamsabadi A, Khalili-Tehrani P, Stewart JP, Taciroglu E. Validated simulation models for lateral response of bridge abutments with typical backfills. Journal of Bridge Engineering. 2009 Jul 13; 15(3):302-311. [\[View at Google Scholar\]](#); [\[View at Publisher\]](#).
- [6] Aviram A, Mackie KR, Stojadinović B. Guidelines for nonlinear analysis of bridge structures in California. Berkeley: Pacific Earthquake Engineering Research Center; 2008. UCB/PEER 2008/03. [\[View at Google Scholar\]](#); [\[View at Publisher\]](#).
- [7] GAO Y, LIN L. EFFECTS OF MODELLING PARAMETERS ON THE SEISMIC ANALYSIS OF BRIDGES. In: Gao Yu, editor. Seismic Resistant Structures. 1st ed. Boston: WITPress; 2018. P.185. [\[View at Google Scholar\]](#); [\[View at Publisher\]](#).
- [8] Taherkhani H, Tajdini M, Rezaee Arjroodi A, Zartaj H. Investigation of bridge abutment displacements constructed on piles and geogrid reinforced soil using the finite element method. Scientia Iranica. 2019 Apr 1; 26(2):625-633. [\[View at Google Scholar\]](#); [\[View at Publisher\]](#).
- [9] Xie Y, Zheng Q, Yang CS, Zhang W, DesRoches R, Padgett JE, Taciroglu E. Probabilistic models of abutment backfills for regional seismic assessment of highway bridges in California. Engineering Structures. 2019 Feb 1; 180:452-467. [\[View at Google Scholar\]](#); [\[View at Publisher\]](#).
- [10] Zampieri P, Simoncello N, Pellegrino C. Seismic capacity of masonry arches with irregular abutments and arch thickness. Construction and Building Materials. 2019 Mar 20; 201:786-806. [\[View at Google Scholar\]](#); [\[View at Publisher\]](#).
- [11] Kun C, Chou N. Estimation of response of skewed bridges considering pounding and supporting soil. Engineering Structures. 2019 Apr 1; 184:469-479. [\[View at Google Scholar\]](#); [\[View at Publisher\]](#).
- [12] Zakeri B, Zareian F. Design of bridges with skewed abutments for a target tolerable seismic loss. Engineering structures. 2018 Jun 1; 164:325-334. [\[View at Google Scholar\]](#); [\[View at Publisher\]](#).
- [13] Kozak DL, LaFave JM, Fahnestock LA. Seismic modeling of integral abutment bridges in Illinois. Engineering Structures. 2018 Jun 15; 165:170-183. [\[View at Google Scholar\]](#); [\[View at Publisher\]](#).
- [14] Nasiri Y, Zarfam P. Estimating the Loading Pattern Factor of Modal Pushover Analysis (MPA) for Integrated Bridges Using IDA Responses. Journal of Seismology and Earthquake Engineering. 2018 Mar 7; 19(2):163-169. [\[View at Google Scholar\]](#); [\[View at Publisher\]](#).
- [15] Zheng Y, McCartney JS, Fox PJ, Shing PB. Acceleration Response of a Geosynthetic Reinforced Soil Bridge Abutment under Dynamic Loading. Geotechnical Special Publication. 2018 Jan 07; 2018(GSP 293):1-9. [\[View at Google Scholar\]](#); [\[View at Publisher\]](#).
- [16] Meteş E, Toduşi L, Petzek E. INTEGRAL BRIDGES-LENGTH LIMITATION, TRANSITION SLABS, EXAMPLES. 6th INTERNATIONAL CONFERENCE Contemporary achievements in civil engineering . SERBIA: 2018. P.17-24. [\[View at Google Scholar\]](#); [\[View at Publisher\]](#).
- [17] Aviram A, Mackie KR, Stojadinovic B. Effect of abutment modeling on the seismic response of bridge structures. Earthquake Engineering and Engineering Vibration. 2008 Dec 1;7(4):395-402. [\[View at Google Scholar\]](#); [\[View at Publisher\]](#).
- [18] Karantzakis M, Spyrakos CC. Seismic analysis of bridges including soil-abutment interaction. InProceedings of the12th world congress on earthquake engineering. New Zealand: TBI; 2000. Paper (No. 2471). [\[View at Google Scholar\]](#); [\[View at Publisher\]](#).
- [19] Kim SJ, Elnashai AS. Seismic assessment of RC structures considering vertical ground motion. United States: Mid-America Earthquake Center CD; 2008 December 19. Mid-America Earthquake Center CD Release 08-03. [\[View at Google Scholar\]](#); [\[View at Publisher\]](#).
- [20] Kim SJ, Holub CJ, Elnashai AS. Analytical assessment of the effect of vertical earthquake motion on RC bridge piers. Journal of Structural Engineering. 2010 Aug 25;137(2):252-260. [\[View at Google Scholar\]](#); [\[View at Publisher\]](#).
- [21] Imbsen RA. AASHTO guide specifications for LRFD seismic bridge design. United States: American Association of State Highway & Transport Officials, Subcommittee for seismic effects on bridges. 2007. [\[View at Google Scholar\]](#); [\[View at Publisher\]](#).
- [22] Bozorgnia Y, Niazi M, Campbell KW. Characteristics of free-field vertical ground motion during the Northridge earthquake. Earthquake spectra. 1995 Nov 1;11(4):515-525. [\[View at Google Scholar\]](#); [\[View at Publisher\]](#).

[Scholar](#); [View at Publisher](#).

[23] Bozorgnia Y, Niazi M, Campbell KW. Relationship between vertical and horizontal response spectra for the Northridge earthquake. In *Memorias, XI World Conference on Earthquake Engineering*. Mexico: 1996. Paper No. 893. [View at Google Scholar](#); [View at Publisher](#).

[24] Abeysinghe RS, Gavaise E, Rosignoli M, Tzaveas T. Pushover analysis of inelastic seismic behaviour of Greveniotikos bridge. *Journal of Bridge Engineering*. 2002 Mar 01;7(2):115-126. [View at Google Scholar](#); [View at Publisher](#).

[25] Cahill NE, Heyland DK. Bridging the guideline–Practice gap in critical care nutrition: A review of guideline implementation studies. *Journal of Parenteral and Enteral Nutrition*. 2010 Nov 19;34(6):653-659. [View at Google Scholar](#); [View at Publisher](#).

[26] Mitoulis SA. Seismic design of bridges with the participation of seat-type abutments. *Engineering Structures*. 2012 Nov 1; 44:222-233. [View at Google Scholar](#); [View at Publisher](#).

[27] Wilson JC, Tan BS. Bridge abutments: formulation of simple model for earthquake response analysis. *Journal of Engineering Mechanics*. 1990 Aug 01;116(8):1828-1837. [View at Google Scholar](#); [View at Publisher](#).

[28] Poulos HG, Davis EH. *Elastic solutions for soil and rock mechanics*. New-York: John Wiley; 1974. [View at Google](#)

[Scholar](#); [View at Publisher](#).

[29] Shattarat NK, Symans MD, McLean DI, Cofer WF. Evaluation of nonlinear static analysis methods and software tools for seismic analysis of highway bridges. *Engineering Structures*. 2008 May 1; 30(5):1335-1345. [View at Google Scholar](#); [View at Publisher](#).

[30] Kramer SL. Performance-based earthquake engineering: opportunities and implications for geotechnical engineering practice. *Geotechnical Earthquake Engineering and Soil Dynamics Congress IV*. California: ASCE; 2008. pp. 1-32. [View at Google Scholar](#); [View at Publisher](#).

[31] Anon. (2008). "Road and rail bridge design codes in earthquake." Publication 463. [View at Google Scholar](#); [View at Publisher](#).

[32] Somerville PG, Smith NF, Graves RW, Abrahamson NA. Modification of empirical strong ground motion attenuation relations to include the amplitude and duration effects of rupture directivity. *Seismological Research Letters*. 1997 Jan 1; 68(1):199-222. [View at Google Scholar](#); [View at Publisher](#).

[33] Erhan S, Dicleli M. Effect of dynamic soil–bridge interaction modelling assumptions on the calculated seismic response of integral bridges. *Soil Dynamics and Earthquake Engineering*. 2014 Nov 1; 66:42-55. [View at Google Scholar](#); [View at Publisher](#).